4M.2

MESOSCALE FORCING OF MARINE ATMOSPHERIC BOUNDARY LAYER CLOUDS ALONG THE U.S. WEST COAST

T. Haack[1]* and M.A. Wetzel[2]

[1]Naval Research Laboratory, Monterey, CA
[2]Desert Research Institute, Reno, NV

1. INTRODUCTION

Low-level stratus clouds, with their substantial impact on the global climate, have been the subject of numerous research efforts that include the compilation of vast, global datasets, extensive field programs, and publications on theoretical, modeling and observational aspects of cloud systems. Many of these works have been motivated by the climatological role stratus coverage plays in the global radiation balance and the need for proper parameterizations of the relevant forcing mechanisms to adequately predict these clouds in global climate models. For these reasons most of the studies are global in nature and tend to be of coarse spatial resolutions so that fine-scale variability and coastal details are often absent.

In the present study, a high-resolution numerical model is employed to investigate the characteristics of low-level clouds over the U.S. West Coast (USWC). Utilizing hourly forecasts from the Navy's Coupled Ocean/Atmospheric Prediction System (COAMPS®[3]; Hodur 1997), four months are selected from each season of 1999 to produce monthly mean properties of low cloudiness such as percent cloud occurrence (CO), liquid water path (LWP), cloud base heights (CBH) and cloud top heights (CTH). The averages reveal seasonal trends and remarkable spatial variability in both the coastal and offshore stratus layer. The relative impacts of the synoptic circulation, oceanic upwelling, and topographic effects upon the clouds are also discussed.

*Stratiform clouds are common along the eastern branch of the North Pacific subtropical high pressure cell, a region frequently characterized by cold sea surface temperatures, weak upward surface fluxes, and moisture confined below a well-defined marine atmospheric boundary layer (MABL) subsidence inversion. Klein and Hartmann (1993) correlate increased stratus cloud amounts over 5 subtropical regions with increased lower tropospheric static stability *S*, where *S* is the difference between the potential temperature at 700 mb and the surface. With stability typically strongest in summer months, the USWC experiences much of its persistent stratus during the warm season (May-September). Other factors linked to increased cloudiness are associated with aspects of the atmospheric circulation and sea surface temperature: stronger subtropical high, greater surface wind speeds, increased subsidence, cold advection all leading to greater cloud amount (Klein 1997).

Coastal cloudiness and especially fog often develop over oceanic upwelling regions along the northern USWC by direct cooling from cold SST, downward surface sensible heat flux combined with an upward latent heat flux. Once condensation has taken place, cloud layers may be maintained by the positive feedback between static stability and longwave radiative cloud top cooling (Klein and Hartmann 1993). Entrainment mixing and warming tends to offset the cooling at cloud top, while long wave warming at cloud base and solar absorption within the cloud can promote decoupling and lead to stratus breakup.

[3] **COAMPS® is a registered trademark of the Naval Research Laboratory**

* *Corresponding author address:* Tracy Haack, Naval Research Lab, Marine Meteorology Division, 7 Grace Hopper Ave, Stop #2, Monterey, CA. 93943-5502; email: haack@nrlmry.navy.mil

In general, inversion capped MABL are not restricted to the warm season as the USWC is under the influence of the subtropical high throughout the year allowing for seasonal changes in its position and strength and intermittent passage of synoptic systems primarily in winter and spring. Monthly mean sea level pressure maps, derived from NCEP reanalyses available at http://www.cdc.noaa.gov, are instructive for showing how the large-scale pressure pattern shifts throughout the year in the area of interest. From an analysis of soundings at three coastal locations, Dorman and Winant (1995) encounter inversions along the California coast 50% of the time in winter, at even greater percentages during the transitional seasons, and a maximum of 95% of the time in summer. When MABL clouds are confined by the inversion, their fine-scale spatial structure and variations in liquid water content greatly influence low-level conditions and visibility.

The ability to examine monthly mean conditions throughout the seasons with the high temporal and spatial resolutions of a mesoscale numerical model permits a broader depiction of USWC marine layer cloudiness than is currently available in the literature. In the next section, a brief model description, the forecasting procedure and cloud averaging method are given. Section 3 describes the monthly mean low cloud conditions from the 9-km COAMPS forecasts over the USWC to determine seasonal trends and patterns in coastal and offshore stratus layers. Validating data and comparisons with observations are provided in Sec 4, and the discussion and conclusions are presented in Sec. 5.

2. METHODOLOGY

Monthly mean cloud characteristics are established for one month in each season of 1999 from COAMPS forecast fields. An initial "cold start" forecast begins with global fields from NOGAPS (Navy Operational Global Atmospheric Prediction System; Hogan et al. 1991) at 00 UTC October 1998 followed by successive 12 hour-long COAMPS forecasts for the triply nested model domain. Every 12 hours the wind, temperature and water vapor fields are incrementally updated with standard "automated data processing" observations that are quality controlled (Baker 1992) and analyzed on 16 pressure levels with a multivariate optimum interpolation technique described by Barker (1992). Outer boundary conditions are supplied by NOGAPS every 6 hours and inner grids are one-way interactive. A Cressman analysis is done on rawinsonde temperatures and dew points to obtain dew point depression corrections. After removing supersaturation, these increments are interpolated to the model levels, added to the previous 12-hr forecast, and the updated dew point temperatures are converted back to mixing ratio of water vapor. Mixing ratios of cloud liquid water (q_c) and three other prognostic moisture variables (raindrops, snow and ice) are carried forward from the previous forecast.

Cloud processes are treated explicitly in COAMPS with a bulk water type model (Rutledge and Hobbs 1983). In this scheme particles of cloud water are assumed to be monodispersed and thirteen parameterization equations govern the transfer of water substance between phases. Cloud water forms by condensation when the air is saturated with respect to water and is depleted by evaporation to vapor, or by collision and collection with other water particles to form raindrops. Auto conversion to raindrops is set at a threshold value of 1 g kg^{-1}, which allows for formation of larger rain droplets but limits the production of drizzle. COAMPS contains neither a drizzle parameterization nor a convective parameterization at grid resolutions less than 10 km.

The COAMPS inner domain is shown in Fig. 1 labeled with points of interest and geographical locations mentioned in the text. The vertical grid distribution includes 30 levels with a minimum spacing of 10 m at the surface, 11 levels below 1.6 km, and the model top at ~31 km. In this study we consider the characteristics of low clouds that are typically within the MABL and hence, restrict the averages to clouds with tops less than 2 km. The averages are obtained from the 3-dimensional fields of q_c. Cloud base (CBH) and cloud top heights (CTH) are determined by vertically sampling model profiles from the surface to 2 km to find the heights where q_c falls above and below a lower limit of 10^{-3}g kg^{-1}. If a low cloud layer is found, the cloud counter at that grid point is incremented to obtain percent cloud occurrence (CO), and a density weighted q_c is vertically integrated yielding the liquid water path (LWP) below cloud top. These quantities are computed for four selected months

in 1999: January, April, July and October, which are each chosen as representative of a season. The averages are made up of COAMPS hourly output from 12-hour forecasts spanning an entire month; and so the mean at any grid point contains 744 values in all months except April, which contain 720 values.

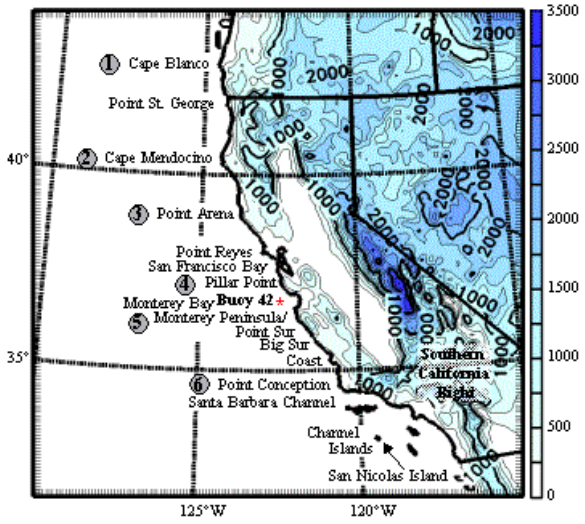

Fig. 1. COAMPS USWC 9-km inner grid with terrain height shaded (m). Six topographic promontories are labeled with numbers.

Haack et al. (*to appear in MWR*) document average surface forcing and flux fields obtained from COAMPS 1999 USWC forecasts for the same four months presented here. While that study focuses on conditions at low-levels, here we address the mean cloud characteristics from COAMPS 9-km inner grid forecasts. In many instances references are made to the averages shown in the earlier paper, and so we reproduce two of those figures here (Figs. 3 and 4). The high-resolution forecasts provide sufficient mesoscale detail and domain coverage to investigate offshore, cross-shore and along-shore stratus variability in addition to the impact of the USWC topography on the low-level cloud field.

3. MONTHLY AVERAGED LOW CLOUD CHARACTERISTICS

The year 1999 is considered a moderate La Niña year with cool SST anomalies in the equatorial Pacific waters that produce blocking high pressure in the eastern Pacific. In addition to the expected cooler SST, the 1999 subtropical high was stronger and positioned farther to the northeast than normal. The enhanced pressure gradients created faster low-level wind speeds offshore of Oregon and northern California in winter and spring of 1999, and diminished wind speeds along southern California throughout the year. The La Niña conditions in this region: a strengthened subtropical high, faster surface winds, and cooler SST, all tend to generate greater low cloud amount and increased overcast conditions (Klein et al. 1995, Klein 1997). This assertion is confirmed by comparing ISCCP (International Satellite Cloud Climatology Project) long term monthly mean cloud amounts to the 1999 monthly means (available at isccp.giss.nasa.gov), which show broader regions of greater low cloud amount along the USWC and offshore waters in 1999. The ISCCP data provide 3-hourly, global coverage of satellite cloud products at much coarser resolution (280 km) than those presented here for the USWC.

Several mechanisms contribute to horizontal variability in cloud characteristics. The baroclinic slope of the marine layer, large-scale subsidence, and low-level divergence are determined by the position and strength of the subtropical high and thermal low. This large scale forcing leads to cross-shore variations in cloud layer depths, and fine-scale cloud features are driven by local surface wind patterns associated with sea/land breeze flows. Horizontal spatial variations in the surface sensible and latent heat, determined in part by the SST pattern, create differences in surface layer heat and moisture transport. Cloud layer thermal instabilities are generated by short- and longwave radiation. And the resultant turbulent structures, along with the microphyscial processes of condensation and evaporation, impart cloud layer instabilities and small-scale mixing that are inherently inhomogeneous and feedback nonlinearly to the cloud field. Each of these factors operates in conjunction with topographic forcing, which can elevate/deepen or lower/thin cloud layers to varying degrees throughout the seasons.

The USWC orography influences the spatial structure of marine layer low clouds by forcing the flow over and around topographic features, which can raise (lower) MABL depths above (below) levels of condensation. Ström et al. (2001) describe the degree to which the MABL is blocked by the coastal orography, based mainly upon stratification, terrain height and wind

speed. Weak stratification, low mountains, and fast winds are prone to forcing the MABL up and over the coastal orography, while strong stratification, high terrain and weaker winds more effectively channels the flow along rather than over coastal mountains.

Channeled flow moving faster than the propagation speed of internal gravity waves may be approximated by the hydrodynamics principles of a two-layer fluid. In this simplified framework, continuity requires that the depth and speed of the MABL vary with each bend in the coastal barrier, thinning and quickening around concave bends, thickening and slowing at convex ones (Winant et al. 1988). Hence, topographically driven stratus is more likely to form where the MABL has been lifted or deepened and dissipate more readily where the MABL is shallow or suppressed. Additionally, when the depth of the MABL is near the height of the coastal mountain, lee waves can further strengthen and lower the MABL inversion as flow above the marine layer descends the terrain. If capped by a low, strong inversion, a fast moving MABL typically contains hydraulic signatures, and a predisposition for clouds/clearing in certain locations, which are anchored to topographic features. In examining the monthly trends of the four low cloud parameters forecast by COAMPS, we consider topography and several other possible synoptic and mesoscale forcing mechanisms in cloud development, dissipation and variability.

3.1 *Surface forcing*

Strong and persistent northwesterly winds in the spring generate oceanic upwelling along the coast. It has a pronounced signature in the July and October 1999 average SST fields between Cape Blanco and San Francisco (Fig. 3c and 3d). Consequently, the cloud averages undergo a marked transition between April and July. The percent cloud occurrence (CO) (Fig. 2, column 1) nearly doubles along the central CA coast. By October the integrated cloud liquid water (LWP) (Fig. 2, column 2) has increased substantially over and especially downwind of the primary upwelling center, which shifts to the north from summer to fall. In addition to the strong subsidence typical of summer and fall, the cold SST and negative surface sensible heat fluxes (Fig. 4c and 4d) all support the development of low-level clouds along the coast. Interestingly, the coldest coastal SST in April, July and October are coincident with *minima* in coastal low-clouds.

Klein et al. (1995) study correlations of summertime low-level clouds in the Northeast Pacific with many local and large-scale variables, finding in particular that cloudiness is best correlated (negatively) with SST approximately 500-600 km upwind. Likewise for the 1999 averages, cloudiness in all months but January is also greater downwind, rather than over, regions having the coldest coastal SST (Fig. 2a, column 1 and Fig.). Further, this negative correlation between low clouds and SST suggests that the warm SST upwind and offshore of Cape Blanco in July may be contributing to the low percent CO and LWP extending ~650 km downwind from this region (Fig. 2c, columns 1 and 2). Downwind of upwelling, increased cloud amounts extend the length of the coast to the Southern CA Bight (~300 km in April, ~700 km in July and ~1000 km in October), despite transitions in surface sensible heat flux and abrupt variations in low-level wind speed. As pointed out by Pilie et al. (1979), dissipated cloud layers are more favorable to reformation by being left cooler than their upwind state.

In many coastal locations, cloud bases (CBH) and tops (CTH) (Fig. 2, column 3 and 4) are also responding to the underlying surface forcing imposed by the SST. Where coastal SST are warm, such as north of Cape Blanco in July, sensible and latent heat fluxes are more unstable (Fig. 4c) leading to an increase in MABL turbulent mixing and cloud layers that are about twice as deep as over nearby upwelling locations. Excluding the north coast in January and April, which are strongly impacted by synoptic storms, coastal regions with the coldest SST all have CBH and CTH that are lower over and well downwind of these locations, such as offshore of San Francisco in January, the finger of cold coastal SST in April, and the north coast's upwelling in July and October.

Inhomogeneities in the cloud field may be introduced by fine-scale variations in the SST fronts and eddies. Upwelling during the warm season enhances these SST gradients generating small-scale spatial variations in the surface fluxes in addition to perturbing the low-level wind field. Note for example the two lobes of lower CBH and CTH in October extending southwestward from Cape Blanco and Cape

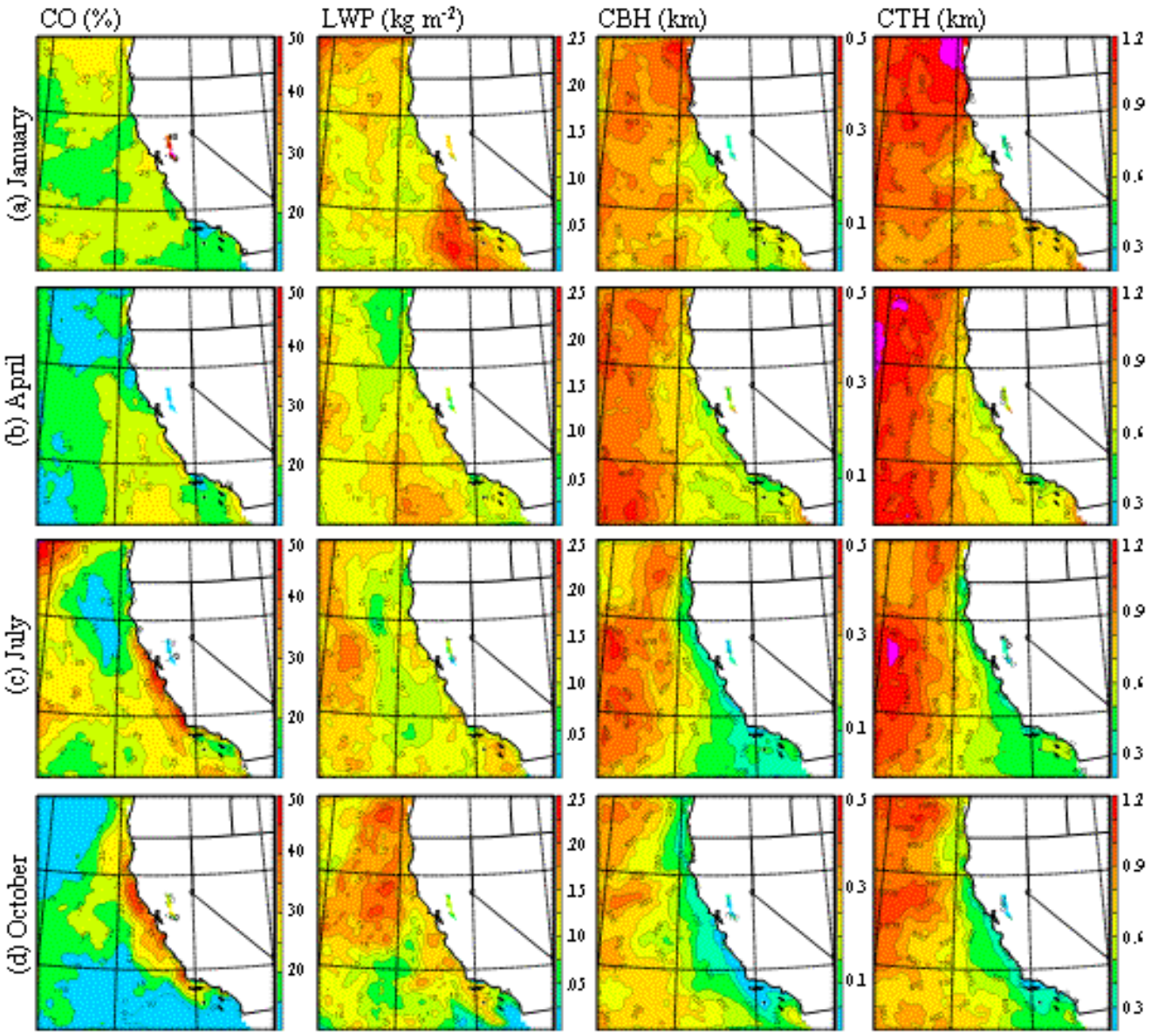

Fig. 2. COAMPS monthly averaged color shading of cloud fields: cloud occurrence (%) in column 1, liquid water path (kg m^{-2}) in column 2, cloud base height (km) in column 3, and cloud top height (km) in column 4 for (a) January, (b) April, (c) July, and (d) October 1999.

Mendocino, two regions having the coldest SST, largest downward sensible heat flux and weak upward latent heat flux (Figs. 3d and 4d). Colder temperatures raise the saturation specific humidity and a stable sensible heat flux suppresses turbulent mixing so that the clouds are typically lower in height and more stratiform in appearance. Additionally October coastal wind speeds are slower than July (Fig. 3d), allowing SST gradients to have a greater impact on the cloud field.

3.2 *Large-scale forcing*

While the atmosphere tends to be both cooled and moistened over upwelling regions, coastal overcast conditions also depend upon the large-scale pressure pattern, in particular the

strength and position of the subtropical high and during the warm season, of the thermal low over the continental U.S. southwest. During the summer, CA's central and southern coasts are in the subsiding eastern branch of the subtropical high pressure cell that suppresses the marine layer, strengthens the inversion and increases the lower tropospheric static stability, all features associated with increased cloud amounts (Klein 1997). Consequently, coastal clouds are more frequent from Cape Mendocino south (Fig. 2, column 1) where isobars are aligned at an angle with the coastline producing greater offshore flow above the marine layer. Moreover, the predisposition for upper-level subsidence yields shallow stratus layers as shown by the wedge of lower CBH and CTH extending from roughly Pt. Arena south during all seasons (Fig. 2, columns 3 and 4). The shallowing increases from summer through fall revealing the impact of greater offshore flow in suppressing cloud depths. Subsidence appears to be the dominant factor in the mean patterns of CBH and CTH, since heights remain low well downwind of upwelling centers over increasingly warmer SST and greater upward surface fluxes (Figs. 3 and 4).

While Klein (1997) finds a positive statistical correlation between low cloud amount and lower tropospheric static stability, a substantial increase in subsidence can actually reduce cloud amounts and promote clearing by lowering inversion heights below levels of condensation. In steady-state modeling simulations of summertime USWC stratus, Wang et al. (1993) for example found that cloud cover decreases by 30% when the large-scale divergence is nearly doubled. For subsidence to contribute positively to cloud amounts it must be balanced by either an increase in surface moisture or decrease in surface temperature, both of which occur over colder water typical of the warm season's coastal upwelling.

The abatement of synoptic storms, increased subsidence and coastal upwelling cause a gradual transition from a coast parallel slope in CBH and CTH in January to the coast perpendicular one in July and October. The slope is much steeper in the northern coastal region with July displaying the largest gradient of the four months. Here cloud depths lower from 1 km to 400 m over a ~150 km cross-shore distance. The north coast also experiences the greatest transition in CBH and CTH throughout the year. Cloud tops in October near Cape Blanco are half the January heights. This region is subject to large seasonal variability being in the path of wintertime storms and then over the coldest upwelling in the fall.

Simon (1977) examines the relationship between USWC cloudiness and surface winds in July. In that study, a combination of offshore westward return flow around the subtropical high and near-shore, cross-isobaric flow toward low pressure drives the inversion below lifting condensation levels along ~125°W longitude creating a "minimum cloudiness line". This feature is apparent in the July 1999 averages as both the percent CO and LWP (Fig. 2c, columns 1 and 2) are minima along the direction of the flow between 127° and 125°W longitude. However, this region is also downwind of locally warmer SST indicating that both the surface and large-scale forcing are both likely influencing July's cloud patterns. Indeed, Klein (1997) finds that no single parameter can predict variations in daily cloud amount since it tends to be significantly correlated with many variables.

April's offshore low cloudiness may be largely dominated by the large-scale wind forcing, which displays an elongated maximum between Cape Mendocino and Point Conception along 125°W longitude (Fig. 3b). Low-level speed divergence upwind of the maximum can shallow the marine layer producing the low cloud amounts near (42ºN, 127ºW) (Fig. 2b, column 1). When clouds do occur in this northern location, they tend to be deep, short-lived convective clouds associated with passing short waves during the first two weeks of April. Likewise, low-level speed convergence downwind of the maximum can elevate MABL depths, so that clouds are more prevalent over southern latitudes (33ºN, 123ºW) in April. In spring, the relatively fast wind speeds tend to overwhelm the more subtle features in the other surface forcing fields.

3.3 *Topographic and coastal forcing*

Mesoscale structure imparted by coastal baroclinity and topographic influences extend approximately a Rossby radius of deformation l_R from the coastline (Ström et al. 2001). While this distance depends upon the Brunt-Väisälä frequency and the height of the topography, its inverse relationship to latitude causes l_R to be ~30% larger at the southern boundary (~30ºN)

compared to northern one (~45ºN). In summer and fall l_R also tends to be larger in the south due to greater stratification. Typical values of l_R can range from 50 to 100 km. In many of the coastal cloud fields, we note a fanning or broadening in the patterns with decreasing latitude that is consistent with the gradual increase in the Rossby radius of deformation.

A deep, weakly defined MABL impinging on the coast will be lifted over the steep coastal topography during forceful eastward flow of winter. And hence, January cloud top and base heights are a maximum at the coast within the northern USWC storm path. However, blocking is more likely during the warm season when fast-moving northwesterly flow is confined by a well-defined inversion below the height of the adjacent coastal mountains. Under those conditions, spatial variations in cloud amounts and cloud top height are influenced by the hydrodynamics of a relatively dense, inversion-capped MABL modulated by the variations in the topography.

Hydraulic behavior is exhibited in the MABL by compression waves and expansion fans at the six coastal promontories (see Fig. 1b) along the USWC (Winant et al. 1988, Dorman et al. 2000, Burk and Haack 2000, Haack et al. 2001). Further, large-scale subsidence typical of the warm season also enhances the hydraulic control of the MABL by strengthening and lowering the inversion. Consequently, topographic forcing becomes more pronounced from Pt. Arena south where the California coastline turns away from the flow. The elevation of the MABL by compression waves tends to promote cloud development along headlands as the inversion is raised above the level of condensation. Alternatively, clearing in the lee occurs where the inversion height is lowered below the level of condensation in expansion fan regions.

Examination of the percent CO (Fig. 2, column 1) reveals that during July and October local increases in cloudiness occur upwind of capes and points. Cloud top heights in July also contain the imprint of terrain forcing being shallower downwind of these topographic features, which, in addition to expansion fan thinning, are also locations of localized leeside downsloping. The LWP shows no distinct topographic signature, as this vertically integrated quantity is sensitive to variations in several cloud features including its depth, thickness and liquid water content.

The effect of coastal baroclinity on clouds is discussed by Koracin and Dorman (2001) who link diurnal trends in near-surface divergence to those in the satellite-derived albedo (a proxy for cloud amount). They find a sharp increase in divergence shortly after sunrise coinciding with an equally sharp drop in 'cloud' albedo. Regions with greater divergence are expected to be less cloudy as MABL depths compensate by lowering below condensation levels. Expansion fans exhibit the greatest diurnal increase in divergence and thus are more likely to clear. Diurnal trends are not considered in the present study since the averages are comprised of hourly forecasts over the full 24-hr diurnal cycle. However, from patterns in percent CO (Fig. 2, column 1), portions of the expansion fan regions (south of Cape Mendocino, Monterey Peninsula/Pt. Sur, and Pt. Conception) do exhibit consistently fewer clouds than are present in the upwind flow while all six promontories tend to have a localized windward increase in cloudiness. Although topographic forcing readily generates and maintains clouds at capes and points, expansion fan clearing is less evident relying upon a combination of additional diurnal factors (low-level divergence, solar warming, lee wave subsidence) to compensate for the cool, saturated MABL arriving from upwind.

4. CONCLUSIONS

Monthly mean properties of low-level cloudiness over the Eastern Pacific and U.S. West Coastal waters are derived from 9-km resolution COAMPS forecasts of cloud liquid water mixing ratio. Hourly fields are averaged for one month in each season of 1999 (January, April, July and October) to obtain percent cloud occurrence, integrated liquid water path, cloud base and top heights. The seasonal trends inferred from the monthly averages indicate a shift in the mean cloud field throughout the year as thicker and deeper clouds along the Pacific Northwest's storm track are replaced by shallow clouds of higher liquid water content along the coast. The cloud patterns respond to both synoptic and mesoscale forcing mechanisms associated with changes in the orientation of the large-scale pressure gradient, upper-level subsidence and low-level divergence, the

establishment of a sloping marine atmospheric boundary layer (MABL) inversion interacting with coastal topography, and the changes in the underlying surface forcing.

The averages display substantial mesoscale variability, which in some cases can be linked to the monthly mean pattern in sea surface temperature (SST). In all months but January, an increase in low-level coastal clouds occurs predominately downwind of, rather than over the coldest coastal SST. Over and downwind of the primary upwelling centers in July and October, the mean cloud field has much lower cloud bases and tops than over the warmer upwind or offshore SST. These lower cloud base and top heights extend well offshore in October. With wind speeds having diminished significantly from July, the SST and surface fluxes play a greater role in the October cloud forcing. In contrast, strong winds dominate in April overwhelming the subtle variations imparted by the SST. April cloud amounts are greater (lesser) downwind (upwind) of the low-level wind maximum driven by the convergent (divergence) patterns in the wind field.

During the inversion-capped months of July and October, the shallow MABL is channeled along and more strongly blocked by the coastal mountain ranges. The influence of variations in the coastline and coastal orography becomes much more pronounced. Hydraulic control of a fast moving marine layer promotes higher cloud amounts and liquid water contents upwind of promontories as MABL tops become lifted above condensation levels by headlands and points as opposed to downwind where the MABL is thinned. The topographic forcing extends approximately a Rossby radius of deformation from the coast (~50-100 km) within which the steep slope of the marine layer toward the coast creates sharp cross-shore gradients in cloud base and top heights. The general turning of the coastline away from the flow from Cape Mendocino south produces a successively lower cloud deck by enhanced divergence of low-level flow and subsidence aloft. The month-to-month variation in cloud patterns and magnitudes are instructive for ascertaining seasonal trends and mesoscale spatial inhomogeneities in relation to the different large-scale, surface and topographic forcing mechanisms.

Acknowledgements. This research was supported by the Office of Naval Research through Program Element 0601153N and 0602435N. Computational support was provided by the Department of Defense Shared Resource Center, U.S. Army Corps of Engineers Waterways Experiment Station HPC Center.

REFERENCES

Baker, N. L., 1992: Quality control for the navy operational atmospheric database, *Wea. Forecasting*, **7**, 250-261.

Barker, E. H., 1992: Design of the navy's multivariate optimum interpolation analysis system, *Wea. Forecasting*, **7**, 220-231.

Burk, S. D., and T. Haack, 2000: The dynamics of wave clouds upwind of coastal orography, *Mon. Wea. Rev.***, 128**, 1438-1455.

Dorman, C. E., and C. D. Winant, 1995: Buoy observations of the atmosphere along the west coast of the United States, 1981-1990, *J. Geophys. Res.*, **100**(C8), 16,029-16,044.

_____, T. Holt, D. P. Rogers, and K. Edwards, 2000: Large-scale structure of the June-July 1996 marine boundary layer along California and Oregon, *Mon. Wea. Rev.*, **128**, 1632-1652.

Haack, T., S. D. Burk, C. E. Dorman, and D. P. Rogers, 2001: Supercritical flow interaction within the Cape Blanco-Cape Mendocino orographic complex, *Mon. Wea. Rev.* **129**, 688-708.

_____, S. D. Burk, R. M. Hodur: U. S. West Coast surface heat fluxes, wind stress and wind stress curl from a mesoscale model reanalysis. *To appear in Mon. Wea. Rev.*

Hogan, T. H., and T. E. Rosmond, 1991: The description of the U.S. Navy Operational Global Atmospheric Prediction System's spectral forecast model. *Mon. Wea. Rev.*, 119, 1786-1815.

Hodur, R. M., 1997: The Naval Research Laboratory's Coupled Ocean/Atmosphere Mesoscale Prediction System (COAMPS), *Mon. Wea. Rev.,***125**, 1414-1430.

Klein, S. A, and D. L. Hartmann, 1993: The seasonal cycle of low stratiform clouds. *J. Climate*, **6**, 1587-1606.

_____, D. L. Hartmann, and J. R. Norris,1995: On the relationships among low-cloud structure, sea surface temperature, and atmospheric circulations in the summertime northeast Pacific. *J. Climate*, **8**, 1140-1155.

_____, 1997: Synoptic variability of low-cloud properties and meteorological parameters in the subtropical trade wind boundary layer. *J. Climate*, **10**, 2018-2039.

Koracin, D. and C. E. Dorman, 2001: Marine atmospheric boundary layer divergence and clouds along California in June 1996. *Mon. Wea. Rev.*, **129**, 2040-2056.

Pilie, R. J., E. J. Mack, C. W. Rogers, U. Katz, and W. C. Kocmond, 1979: The formation of marine fog and development of fog-stratus systems along the California coast. *J. Appl. Meteor.* **18**, 1275-1286.

Rutledge, S.A., and P.V. Hobbs, 1983: The mesoscale and microscale structure of organization of clouds and precipitation in midlatitude cyclones.VIII: A model for the “seeder-feeder” process in warm-frontal rainbands. *J. Atmos. Sci.*, **40**, 1185-1206.

Simon, R. L., 1977: The summertime stratus over the offshore waters of California. *Mon. Wea. Rev.*, **105**, 1310-1314.

Ström, L., M. Thernström, D. P. Rogers, 2001: Observed dynamics of coastal flow at Cape Mendocino during Coastal Waves 1996. *J. Atmos. Sci.*, **58**, 953-977.

Wang, S., B. A. Albrecht, P. Minnis, 1993: A regional simulation of marine boundary-layer clouds. *J. Atmos. Sci.,* **50**, 4022-4043

Wetzel, M. A., W. T. Thompson, G. V. Vali, S. K. Chai, T. Haack, M. J. Szumowski, and R. Kelly, 2001: Evaluation of COAMPS forecasts of coastal stratus using satellite microphysical retrievals and aircraft measurements. *Wea. Forecasting*, **16**, 588-599.

Winant, C. D., C. E. Dorman, C. A. Friehe, and R. C. Beardsley, 1988: The marine layer off northern California: An example of supercritical channel flow. *J. Atmos. Sci.*, **45**, 3588-3605.

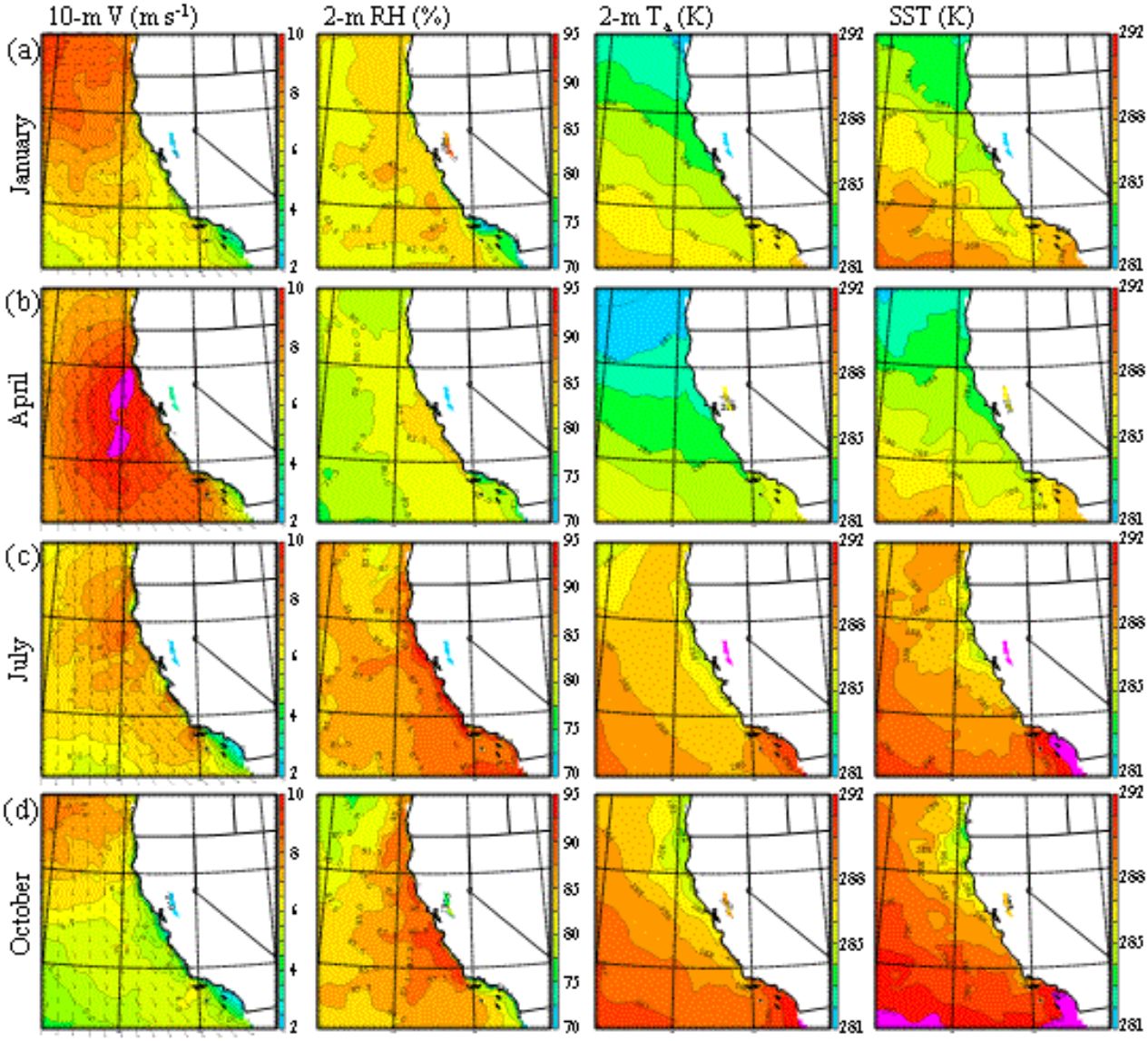

Fig. 3. COAMPS monthly averaged color shading of near surface fields: 10-m winds speed (m s^{-1}) and directional arrows in column 1, 2-m relative humidity (%) in column 2, 2-m air temperature (K) in column 3, and sea surface temperature (K) in column 4 for (a) January, (b) April, (c) July, and (d) October 1999 (reproduced from Haack et al. *to appear in MWR).*

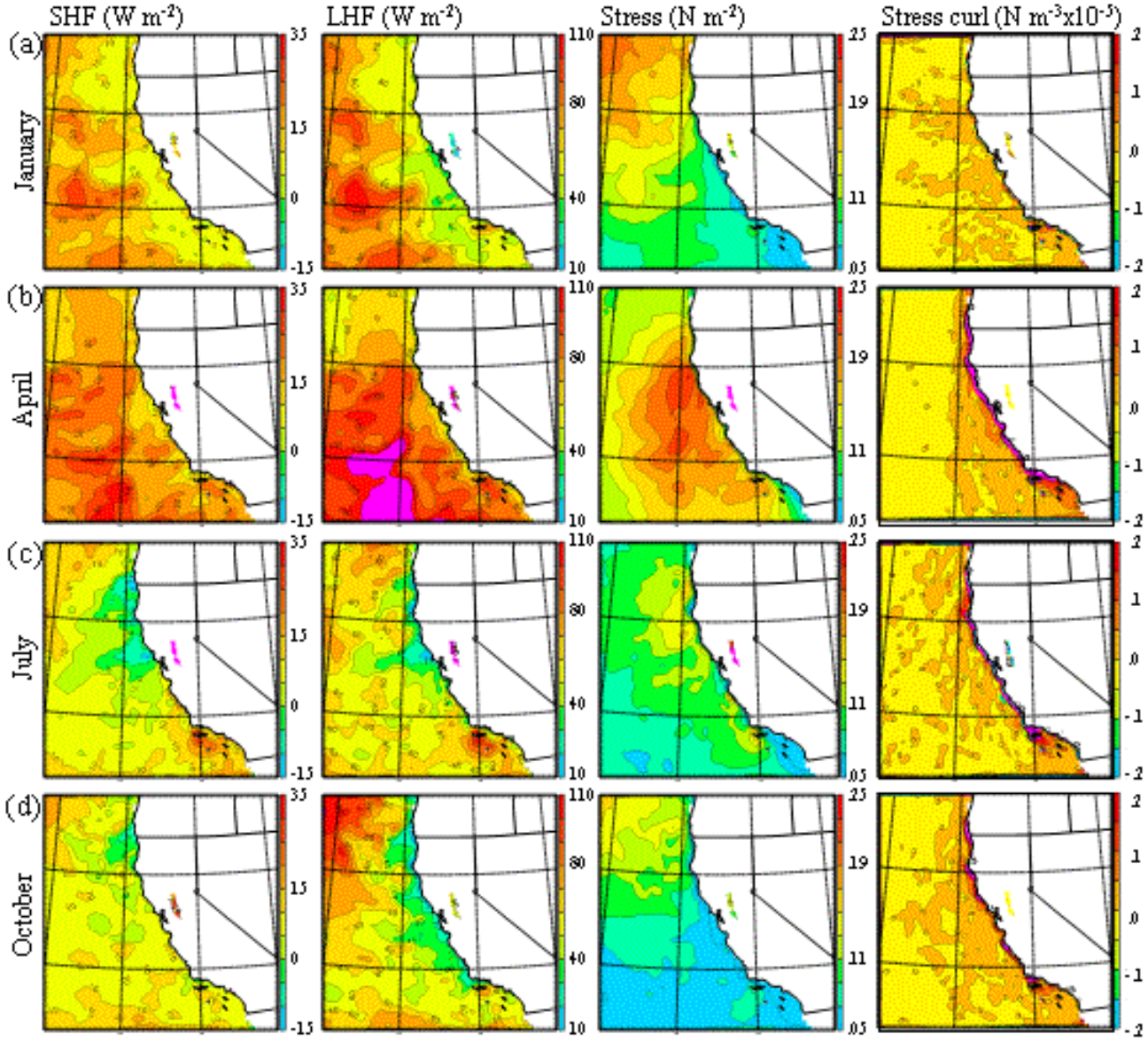

Fig. 4. COAMPS monthly averaged color shading of surface forcing fields: sensible heat flux (W m^{-2}) in column 1, latent heat flux (W m^{-2}) in column 2, surface wind stress (N m^{-2}) in column 3, and wind stress curl (N m^{-3}x10^{-5}) in column 4 for (a) January, (b) April, (c) July, (d) October 1999 (reproduced from Haack et al. *to appear in MWR).*